

Effect of Critical Temperature on the Energy and Exergy of Transcritical Organic Rankine Cycles with Zeotropic Mixture Working Fluids in Low-grade Heat

Jui-Ching Hsieh* and Ding-Xuan Huang**

Keywords: transcritical organic Rankine cycle; zeotropic mixtures; exergy;

ABSTRACT

A thermodynamic analysis model of the transcritical organic Rankine cycle associated with zeotropic mixtures has been developed. This model was employed to investigate the effects of critical mixture temperature on the first and second law efficiencies of thermodynamics, specific power, net-power-to-cost ratio, irreversibility of the components, and exergy loss of the heat source at expander inlet temperatures of 150–190 °C. The results indicate that evaporator irreversibility and exergy loss of the heat source significantly decreased with an increase in the expander inlet temperature and decrease in the mixture critical temperature, which resulted in improved specific power and second law efficiency. However, the condenser irreversibility was increased with a decrease in the mixture critical temperature owing to the effects of condensation pressure for low critical temperature fluid. Based on the analysis, a universal criterion for the temperature difference between the critical temperature and expander inlet temperature on the maximal second law efficiency has been proposed. Finally, the high critical temperature of the mixed fluid is accompanied by a low condensation pressure, resulting in high first law efficiency, low condenser irreversibility and excellent net-power-to-cost ratio.

Paper Received January, 2022. Revised April, 2022. Accepted June, 2022. Author for Correspondence: Jui-Ching Hsieh.

* Associate Professor, Department of Mechanical Engineering, National Chin-Yi University of Technology, Taichung, Taiwan 41170, ROC.

** Graduate Student, Department of Mechanical Engineering, National Chin-Yi University of Technology, Taichung, Taiwan 41170, ROC.

INTRODUCTION

The organic Rankine cycle (ORC) is one of the effective methods for recovering low-grade waste heat to generate electricity. Numerous pure and mixture working fluids and ORC architectures have been proposed in literatures to investigate their effects on ORC performance. The composition of the mixture working fluids were employed to adjust their physical, chemical, environmental, as well as safety-related properties to improve the design parameters of cycle components. Zeotropic mixtures are used as working fluids in the ORC to achieve higher efficiency than that obtained when using pure fluids based on glide matching of temperature profiles in the condenser and evaporator (Wu et al. (2016), Zhou et al. (2016), Zhao et al. (2014), Lecompte et al (2014)). Zhou et al. (2016) indicated that the partial evaporating ORC (PEORC) reduces exergy loss in the evaporator by improving temperature matching between the heat source and the working fluid. Liu et al. (2015) analyzed the effects of the condensing temperature glide on zeotropic mixtures. They found that two maxima appeared in the cycle thermal efficiency, exergy efficiency, and net power output. This occurred at the points where the condensation temperature glide matched the increase in cooling water temperature at two different mole fractions of the more volatile component, when the increase in cooling water temperature was less than the maximum condensation temperature glide of the mixture. Zhou et al. (2017) found that the composition shift characteristic is mainly affected by vapor-liquid equilibrium for a binary zeotropic mixture and by the flow velocity difference between the vapor and liquid phases. A parametric sensitivity analysis of cycle performance indicators, such as energy and exergy efficiencies, cycle irreversibility rate, external heat requirement, and working fluid mass flow rate, is developed at various temperatures and pressures Aghahosseini and Dincer (2013). The critical temperature of the working fluid influences the efficiency of the heat source utilization cycle and losses of exergy in the evaporator and condenser Zhai et al (2016). Heberle et al. (2012) performed a simulation

and analysis of the zeotropic-mixture working fluids R245fa/R227ea and isobutane/isopentane. Wang and Zhao (2010) used three mass fractions of R245fa/R152 to simulate dry, isentropic, and wet working fluids and calculated the ORC efficiency. Moreover, Satanphol et al. (2017) used the Aspen Plus V8.4 simulation software to optimize the performance of the conventional ORC for low-grade heat recovery from pure and zeotropic-mixture working fluids. Hsieh and Cheng (2021) investigated effects of the mixture fluids on exergy and energy with the recuperative TRCs.

Generally, the low-enthalpy heat in geothermal fluids is extracted by using a binary cycle and is converted into electricity. Conventional ORCs are used widely in low-enthalpy geothermal power plants as an effective solution to convert low-grade heat into power. However, conventional ORCs are characterized by high exergy destruction during heat transfer in the evaporator and condenser. The isothermal evaporation destruction and exergy loss can be reduced by employing transcritical organic Rankine cycles (TRCs) Schuster et al. (2010). Chen et al. (2011) indicate that the exergy destruction in a pump, turbine, and condenser decreased with an increase of turbine inlet pressure in the case of a TRC with pure fluid. Algieri and Morrone (2012) considered the influence of internal regeneration on three types of pure working fluids in subcritical and transcritical cycles. Le et al. (2014) found that the highest optimal system efficiency (11.6%) and the highest electrical power (4.1kW) are obtained with R152a and R1234ze as pure working fluids in TRCs, respectively. Moreover, they demonstrated that the critical temperature and normal boiling temperature are the important factors governing the working fluid selection. From the viewpoint of environmental protection, CO₂ is a promising natural working fluid in binary cycles. Moreover, CO₂ and its mixtures have been studied by researchers in the TRC and Brayton cycle (Chen,2012, Mehrpooya,2016, Wu et al.,2017, Wang and Dai,2016). Liu et al. (2020) investigated transcritical cycles by using CO₂/R134a with various mole fractions for waste heat recovery from diesel engines. The experimental results found that the maximum estimations of net power output using CO₂/R134a (0.85/0.15), CO₂/R134a (0.7/0.3), CO₂/R134a (0.6/0.4) and CO₂/R134a (0.4/0.6) are 5.07 kW, 5.45 kW, 5.30 kW, and 4.41 kW, respectively. Recently, operating conditions affecting turbine performance on Brayton cycles and CO₂ transcritical cycle have been investigated Song et al. (2020). Furthermore, Hsieh (2020) conducted an experiment and thermodynamic analysis to investigate the match in operating conditions for the experimental heat extraction of supercritical CO₂ and the CO₂ transcritical power cycle. The results indicated the pseudocritical temperature of the CO₂ in the transcritical cycle should be sufficiently high to approach half the inlet temperature of the expander. Zhi et al. (2019) presented a TRC model that optimized and

predicted thermal and exergy efficiencies by using an artificial neural network (ANN) for low-grade heat recovery.

Wu et al. (2017) investigated transcritical power cycles by using CO₂-based mixtures as working fluids in a geothermal power plant at cooling water temperatures of 10–30 °C. They observed that CO₂-based mixtures were unsuitable for transcritical power cycles at low cooling water temperatures, except R161/CO₂ and R152a/CO₂. Wang and Dai (2016) studied the TRC with CO₂ and ORC with different organic fluids as the bottoming cycles. They found that the performance of the CO₂-TRC was superior to that of the ORC at lower compressor pressure ratios. Dai et al. (2014) found that CO₂-based zeotropic mixtures can improve the thermal performance and lower the operation pressure compared with pure CO₂. Braimakis et al. (2015) developed a map of the maximum exergetic efficiency for subcritical and supercritical ORCs at heat source temperatures ranging from 150 °C to 300 °C corresponding to efficiency ranging from 15% to 40% by using natural fluids and their binary mixtures as working fluids. Although the CO₂-based mixtures have been investigated in the literature, the associated system costs were found to be markedly high because the supercritical pressure of CO₂ is higher than that of the other mixtures. In low-grade heat conversion, most of the exergy is destroyed by the expander, evaporator, and condenser in the binary cycle (Chen (2011), Wu (2016), Le et al (2014)).

According to the aforementioned reviews, exergy destruction during evaporation and condensation can be reduced by using the TRC and mixture fluids, respectively, owing to the excellent temperature match with the heat source in the evaporator and temperature glide in the condenser. Although many pure fluids and their binary mixtures have been studied in the ORC, the previous approaches have limitations in terms of the effects of zeotropic mixtures in TRCs on a reasonable supercritical pressure. In addition to exergy destruction in the components, the exergy loss associated with the outlet temperature of the heat source and the reference temperature cannot be neglected. The heat source outlet temperature in the evaporator depends on the heat source inlet temperature, critical temperature, pinch point, and expander inlet pressure. In particular, the critical point, which is the crucial parameter in the supercritical cycle, can be adjusted based on the mole fraction of the mixture fluids with different critical points to further reduce exergy loss. Hence, the purpose of the present work is to investigate the effects of critical temperature in a TRC system with different mixture working fluids at various expander inlet temperatures. The energy, exergy efficiency and net-output-power-to-cost ratio affected by temperature difference between the expander inlet temperature and critical temperature have been studied.

System model

System description

A schematic of the TRC system was showed in Figure 1. The parameters employed for the analysis of the TRC in the present work were summarized in Table 1. The heat source and cooling temperatures were set in the range of 160–200 °C and 32 °C, respectively. Isentropic efficiency of pump was a key parameter, especially for transcritical cycles Maraver et al. (2014), and it was set as 65% in the present study according to the experimental data reported previously Hsieh et al. (2017).

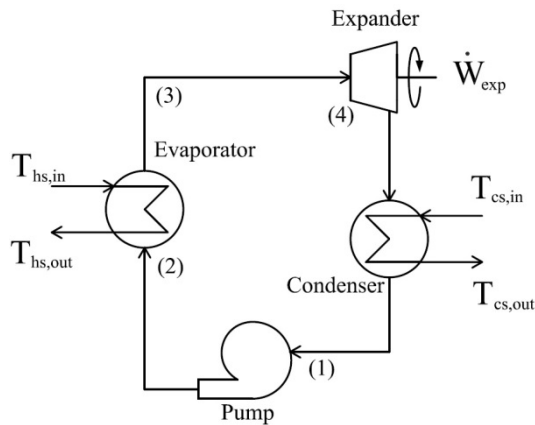


Fig. 1. Schematic of the TRC system.

Table 1. Parameters of the TRC model.

High CT working fluid		R245fa, R600a
Low CT working fluid		R134a, R1234yf
Expander isentropic efficiency	$\epsilon_{exp,is}$	80%
Pump isentropic efficiency	$\epsilon_{pump,is}$	65%
Generator/motor efficiency	$\epsilon_{g,m}$	90%
Pinch point for evaporator	$\Delta T_{pp,eva}$	10 K
Pinch point for condenser	$\Delta T_{pp,cond}$	5 K
Inlet temperature of the expander	$T_{exp,in}$	150–190 °C
Inlet pressure of the expander	$P_{exp,in}$	4.6 MPa
Inlet temperature of heat source	$T_{hs,in}$	160–200 °C
Mass flow rate of heat source	\dot{m}_{hs}	30 kg/s
Inlet temperature of cooling source	$T_{cs,in}$	32 °C
Outlet temperature of cooling source	$T_{cs,out}$	37 °C
Reference temperature	T_0	32 °C

Critical point of zeotropic mixture

Figure 2. shows the typical T–s diagram of the

TRC system using a zeotropic mixture and irreversibility of each component. The temperature glide of the zeotropic-mixture working fluid between the saturated liquid and the saturated vapor lines in the condenser illustrates the non-isothermal process of condensation, which reduces the irreversibility of the condenser. TRCs have the best thermal match between the heat source and the working fluid in the evaporator owing to heating from the subcritical to the supercritical state without isothermal evaporation, which reduces exergy loss of the heat source and irreversibility of the evaporator. The irreversibilities of the components and exergy loss are shown in Fig. 2. by hatched lines. The hatched areas represent exergy destruction of the components and exergy loss of the heat source. From the figure, it can be inferred that most of the exergies are dissipated as $\dot{E}_{hs,loss}$, \dot{I}_{eva} , and \dot{I}_{cond} , which are affected by the outlet temperature of the heat source.

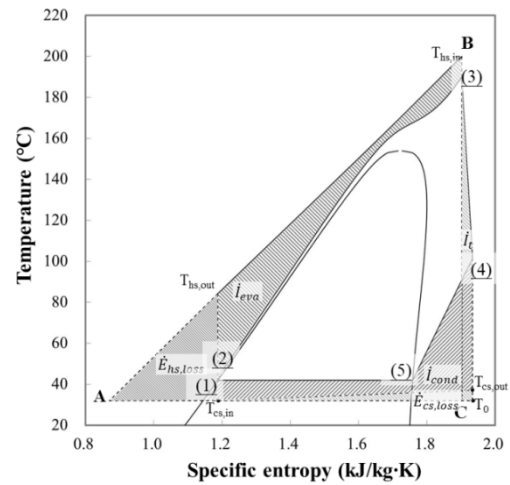


Fig. 2. Exergy of the heat source and irreversibility of the components in the T–s diagram (irreversibility of the pump not shown).

For the TRC system, the critical point is the crucial property of the working fluid because the working fluid must be in the supercritical state before entering the expander. To avoid droplet accumulation owing to a drop in pressure, the inlet temperature and inlet pressure of the working fluid should be sufficiently higher than the critical point to ensure that the working fluid remains in the superheated state during expansion. Additionally, the critical point of the working fluid can be adjusted by changing the mole fraction of the mixture working fluid, as shown in Fig. 3. Variations in the critical points of the mixtures increase with X_f . To achieve safe operation at a reasonable cost in practical systems, we set the supercritical pressure to 4.6 MPa.

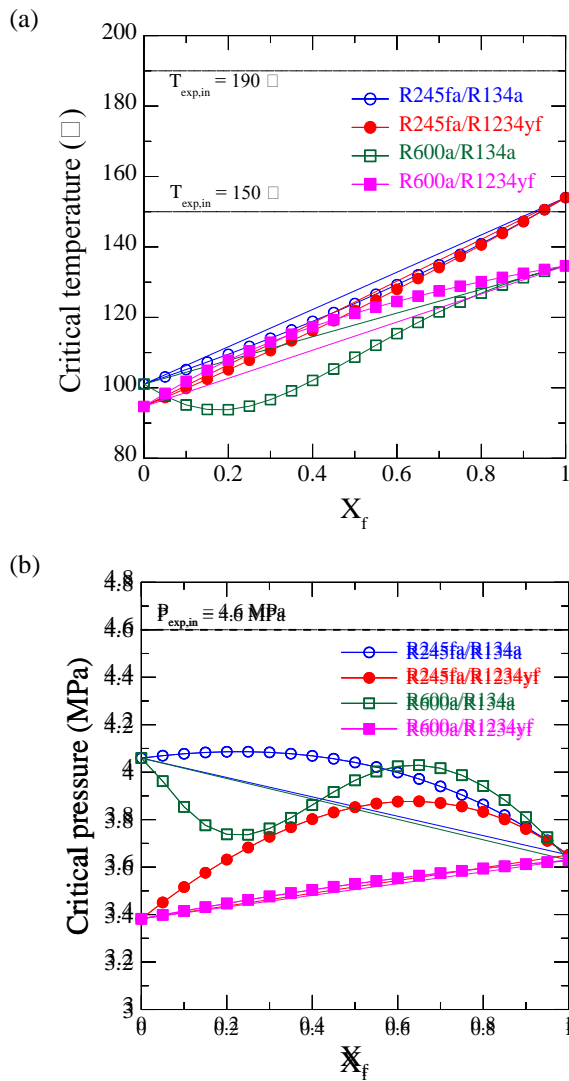


Fig. 3. (a) Critical temperature and (b) critical pressure at various mole fractions of the mixtures.

Condensation temperature glides and condensation pressures

In addition to the effects of the critical temperature of zeotropic mixtures, the condensation pressure should be as low as possible to increase the thermal efficiency of a TRC. The condensation pressure decreased with increased mole fraction of the working fluid with high critical temperature (HCT), as shown in Fig. 4. In the TRC system, temperature glide occurred only in the condenser owing to the phase change of the zeotropic mixture in the two-phase region, which induced a nonisothermal condensation process and affected the condensation pressure. The pinch point temperature of the condenser at the dew point can be expressed as follows:

$$T_5 = T_{cs,out} + \Delta T_{pp,cond} \text{ and } P_1 = P_5$$

Because $T_g \geq \Delta T_{cs}$, the pinch point shifts from dew point to point 1 (the refrigerant outlet of the condenser) in the case of the working fluid.

$$T_1 = T_{cs,in} + \Delta T_{pp,cond} \text{ and } P_5 = P_1$$

The condensation pressure of the zeotropic mixture was affected by the temperature glide, except in the case of R600a/R1234yf. The mole fractions at the temperature glide approached the temperature difference between the inlet and outlet of the cooling source, and they are 0.16/0.84 and 0.96/0.04, 0.19/0.81 and 0.97/0.03, and 0.34/0.66 and 0.95/0.05, respectively, for R245fa/R134a, R245fa/R1234yf, and R600a/R134a.

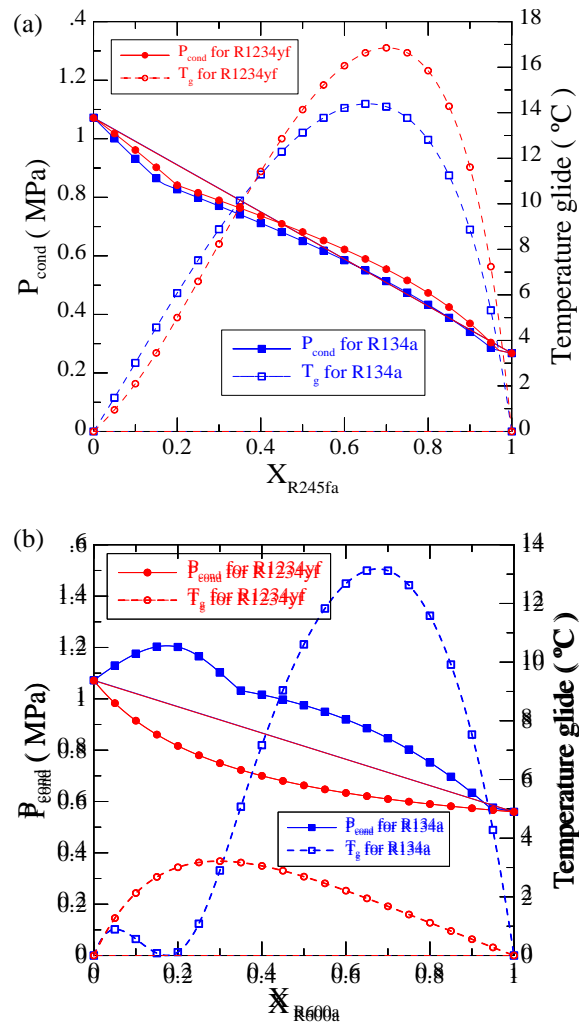


Fig. 4. Condensation temperature glides and condensation pressures for (a) R245fa/R134a and R245fa/R1234yf, (b) R600a/R134a and R600a/R1234yf.

Theoretical analysis

Model assumptions

To simplify the analysis model, the following system assumptions were made: (1) the system is in a steady state; (2) the pressure drop in the evaporator, condenser, and connecting pipes is ignored; moreover, (3) the heat loss of each component and the connecting pipes is ignored.

System thermodynamic analysis

In a TRC system, the pump pressurizes the working fluid to a supercritical state, resulting in a large pressure difference between the evaporator and the condenser. However, the working fluid pump consumes a considerable amount of power from the system generator. The net thermal efficiency (first law efficiency) is estimated by using the following equations:

$$Q_{eva} = \dot{m}_{hs} C_p (T_{hs,in} - T_{hs,out}) \quad (1)$$

$$\eta_{II} = \eta_{th,sys} = \frac{W_{net}}{Q_{eva}} = \frac{W_{exp} - W_{pump}}{Q_{eva}} \quad (2)$$

where W_{net} is the difference between the shaft power produced by the expander and the power consumed by the working fluid pump.

To consider the exergy destruction in the system and its components, we used the continuity equation, energy and exergy balance equation for a control volume in the steady state with no changes in potential and kinetic energy. The corresponding equations are as follows:

$$\sum \dot{m}_{in} = \sum \dot{m}_{out} \quad (3)$$

$$Q + \sum_{in} \dot{m}_{in} h_{in} = \sum_{out} \dot{m}_{out} h_{out} + \dot{W} \quad (4)$$

$$\sum_{in} \left(1 - \frac{T_0}{T_j}\right) Q_j + \sum_{in} \dot{m}_{in} e_{in} = \sum_{out} \dot{m}_{out} e_{out} + \dot{W} + \dot{I} \quad (5)$$

where e , specific exergy, is $h - h_0 - T_0(s - s_0)$. The system and the main components are isothermal, and no exergy is transferred from external heat, so $Q_j = 0$.

The system efficiency and component exergy destructions are evaluated using energy and exergy balance equations. The main design points and components are shown in Fig. 2. The mathematical model of each component is described as follows.

The power consumed and the irreversibility of the pumping process between points 1 and 2 are

$$h_2 = \frac{h_{2s} - h_1}{\varepsilon_{pump,is}} + h_1 \quad (6)$$

$$W_{pump} = \dot{m}_f (h_2 - h_1) \quad (7)$$

$$\dot{I}_{pump} = \dot{W}_{pump} + \dot{m}_f e_1 - \dot{m}_f e_2 = \dot{m}_f T_0 (s_2 - s_1) \quad (8)$$

The irreversibility of evaporation between points 2 and 3 is defined as

$$\dot{I}_{eva} = \dot{m}_f (e_2 - e_3) + \dot{m}_{hs} (e_{hs,in} - e_{hs,out}) = \dot{m}_f T_0 (s_3 - s_2) + \dot{m}_{hs} T_0 (s_{hs,out} - s_{hs,in}) \quad (9)$$

The shaft power of the expander and the irreversibility of expansion between points 3 and 4 are defined as

$$h_4 = h_3 - \varepsilon_{exp,is} (h_3 - h_{4s}) \quad (10)$$

$$\dot{W}_{exp} = \dot{m}_f (h_3 - h_4) \quad (11)$$

$$\dot{I}_{exp} = \dot{m}_f e_3 - \dot{m}_f e_4 - \dot{W}_{exp} = \dot{m}_f T_0 (s_4 - s_3) \quad (12)$$

The irreversibility of condensation between points 4 and 1 can be calculated by

$$Q_{cond} = \dot{m}_f (h_4 - h_1) \quad (13)$$

$$\dot{I}_{cond} = \dot{m}_f (e_4 - e_1) + \dot{m}_{cs} (e_{cs,in} - e_{cs,out}) = \dot{m}_f T_0 (s_1 - s_4) + \dot{m}_{cs} T_0 (s_{cs,out} - s_{cs,in}) \quad (14)$$

The total irreversibility of the TRC system can be summarized as follows:

$$\dot{I}_{tot} = \dot{I}_{pump} + \dot{I}_{eva} + \dot{I}_{exp} + \dot{I}_{cond}$$

Generally, the outlet temperature of the heat source in a TRC evaporator cannot decrease to the reference temperature, and only a part of the exergy from the heat source can be transferred into the TRC system, which can be expressed as

$$\Delta \dot{E}_{hs} = \dot{E}_{hs,in} - \dot{E}_{hs,out} = \dot{m}_{hs} (e_{hs,in} - e_{hs,out}) = \dot{m}_{hs} (h_{hs,in} - h_{hs,out} - T_0 (s_{hs,in} - s_{hs,out})) \quad (15)$$

The exergy loss from the outlet temperature of the heat source in the evaporator to the reference point was evaluated. To investigate the exergy efficiency of the TRC system, the transferred exergy and exergy loss from the heat source in normalization are expressed as

$$1 = \frac{\Delta \dot{E}_{hs}}{\dot{E}_{hs,in}} + \frac{\dot{E}_{hs,out}}{\dot{E}_{hs,in}} = \Psi_{input} + \Psi_{loss} \quad (16)$$

The net exergy transferred from the heat source flows to the net output work and the exergy destruction of the system in normalization is expressed as follows:

$$\Delta \dot{E}_{hs} = \dot{I}_{tot} + \dot{W}_{net} + \dot{E}_{cs,loss} \quad (17)$$

$$1 = \frac{\dot{I}_{tot}}{\Delta \dot{E}_{hs}} + \frac{\dot{W}_{net}}{\Delta \dot{E}_{hs}} + \frac{\dot{E}_{cs,loss}}{\Delta \dot{E}_{hs}}$$

where $\dot{E}_{cs,loss}$ is the exergy discharged from the cooling source.

The second law efficiency and normalized destruction of the system can be determined by

$$\eta_{III} = \frac{W_{net}}{\Delta \dot{E}_{hs}} \quad (18)$$

$$\Omega_{tot} = \frac{\dot{I}_{tot}}{\Delta \dot{E}_{hs}} = \frac{\dot{I}_{pump}}{\Delta \dot{E}_{hs}} + \frac{\dot{I}_{eva}}{\Delta \dot{E}_{hs}} + \frac{\dot{I}_{exp}}{\Delta \dot{E}_{hs}} + \frac{\dot{I}_{cond}}{\Delta \dot{E}_{hs}} = \Omega_{pump} + \Omega_{eva} + \Omega_{exp} + \Omega_{cond} \quad (19)$$

The overall heat transfer coefficient in the evaporator and condenser can be calculated using the logarithmic mean temperature difference (LMTD) method.

The heat transfer rates of the evaporator and condenser are

$$Q_{eva} = (UA)_{eva} \Delta T_{log_eva} \quad (20)$$

$$Q_{cond} = (UA)_{cond} \Delta T_{log_cond} \quad (21)$$

$$UA = (UA)_{eva} + (UA)_{cond} \quad (22)$$

where ΔT_{log} is the LMTD calculated using the

inlet and outlet temperatures of the heat source, cooling source, and working fluids in the evaporator and condenser, respectively; and Q_{eva} and Q_{cond} are the heat transfer rates of the evaporator and condenser, respectively. Furthermore, the overall heat transfer coefficient of the evaporator $(UA)_{eva}$ and the condenser $(UA)_{cond}$ can be calculated by combining Eqs. (1), (13), (20), and (21).

To consider the specific power and the net-power-to-cost ratio, we express the net output power per unit mass flow rate of the heat source and the net output power per unit UA as follows:

$$\xi = \frac{\dot{P}_{net}}{\dot{m}_{hs}} \quad (21)$$

$$\Lambda = \frac{\dot{P}_{net}}{UA} \quad (22)$$

where \dot{P}_{net} is

$$\dot{P}_{net} = (\dot{W}_{exp} \cdot \varepsilon_{g,m}) - \frac{\dot{W}_{pump}}{\varepsilon_{g,m}} \quad (23)$$

Results and Discussion

The mixtures R245fa/R134a, R245fa/R1234yf, R600a/R134a, and R600a/R1234yf were used as working fluids in the TRC. R245fa and R134a, which are nonflammable and have high global warming potential (GWP), are widely used in ORC/TRCs owing to their excellent performance in low-grade heat conversion. R600a and R1234yf are hydrocarbon (HC) and hydrofluoroolefin (HFO), respectively, which have higher flammability and low GWP. Additionally, R245fa and R600a, and R134a and R1234yf have HCT and low critical temperature (LCT), respectively, as presented in Table 2. In the present study, zeotropic mixtures comprising different refrigerants and having various critical temperature values were used to investigate the effects of the relative temperature difference between the expansion inlet temperature and the critical temperature. According to the system thermodynamic analysis in Section 3.2, the model developed herein was solved using MATLAB, and the thermal-physical properties of the working fluid were taken from the National Institute of Standards and Technology (NIST) database REFPROP 9.0 Lemmon et al. (2013).

Table 2. Basic properties of the working fluid.

Working fluids	T_{cri} (°C)	P_{cri} (MPa)	Safety	GWP
R245fa	154.0	3.651	B1	1030
R600a	134.7	3.64	A3	20
R134a	101.1	4.06	A1	1300
R1234yf	94.7	3.38	A2L	4

Validation of analysis model

To validate the thermodynamic analysis model

developed in the present study, the model was solved with the same operating conditions and working fluid as those in Le et al. (2014). R134a in the pure working fluid was computed to compare the net shaft power of the expander, η_I , η_{II} , and \dot{I}_{tot} of the TRC model at the heat source outlet temperature of 70.3 °C. According to the validation results, the relative deviation in the net shaft work, first law efficiency, second law efficiency, and irreversibility are 1.48%, 0.7%, 1.9%, and 0.9%, respectively, as listed in Table 3.

Table 3 Validation of the analysis model for pure working fluid R134a.

	\dot{W}_{net} (kW)	η_I (%)	η_{II} (%)	\dot{I}_{tot} (kW)
Ref. [16]	4.7	14.0	57.0 (η_{ex})	3.4
Present study	4.77	14.1	58.1	3.43
Relative deviation	1.48%	0.7%	1.9%	0.9%

Influences of condensation pressure and temperature glide

For the transcritical cycle with pure fluid, the isothermal process in the evaporator does not occur, but the condensation process in the subcritical state is isothermal. Although a better thermal match between the working fluid and the heat source could be achieved in the evaporator, it depended on the expander inlet temperature and the critical temperature. In the present study, fluids with HCT and LCT were used to create the mixture fluids that were employed to investigate the effects of the critical temperature of the mixtures on the TRC system performance and exergy efficiency. The system efficiency (η_I and η_{II}), specific power (ζ), exergy destruction (Ω_{tot}), and exergy loss (Ψ_{loss}) for the zeotropic mixtures were examined through the mole fraction of the mixtures and various inlet expander temperatures, as shown in Fig. 5.

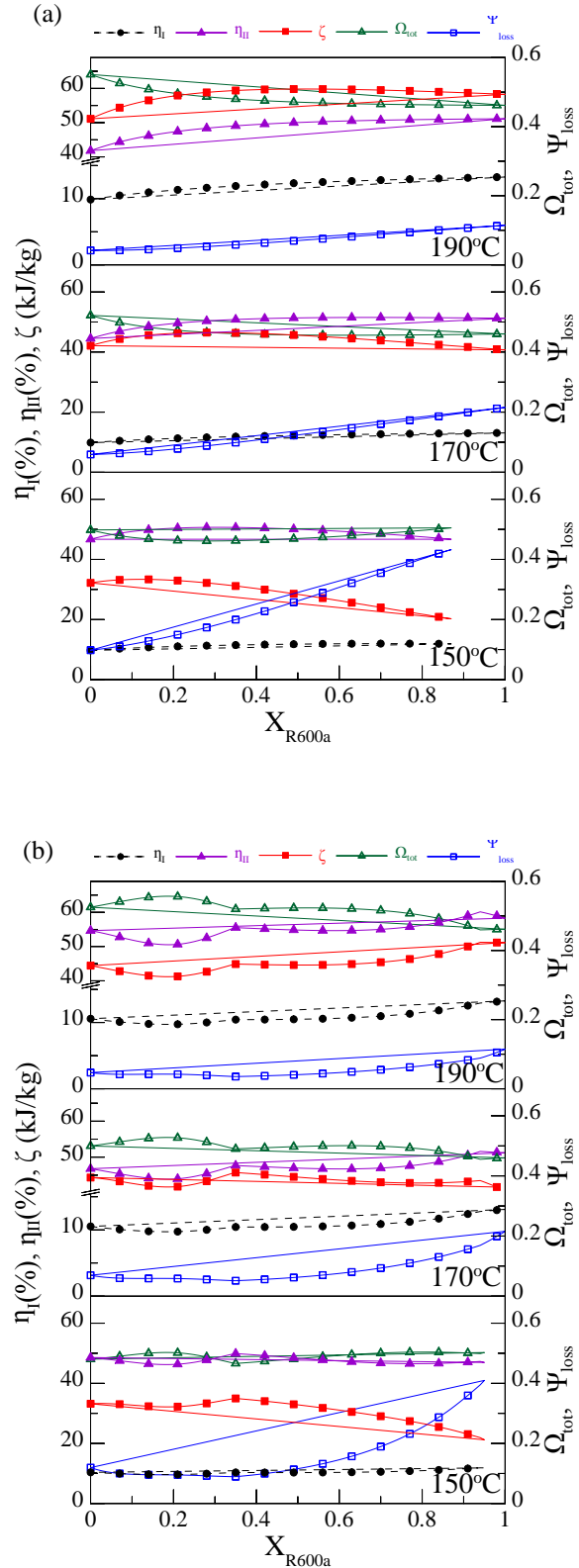
Because the condensation temperature glide was smaller than the temperature difference between the inlet and outlet of the cooling source (as shown in Fig. 4(b)), the performance of R600a/R1234yf was not affected by the temperature glide. Figure 6 shows that η_{II} , ζ , and Ψ_{loss} of R600a/R1234yf improved significantly with the increase in $T_{exp,in}$. This was because Ψ_{loss} significantly decreased with an increase in $T_{exp,in}$, resulting in improved ζ and η_{II} . Ψ_{loss} associated with the outlet temperature of the heat source was as low as possible to obtain an excellent thermal match between the heat source and working fluid. Meanwhile, Ψ_{loss} can be reduced by increasing the proportion of LCT in the mixture at the given $T_{exp,in}$. However, ζ and η_{II} at $X_{R600a} < 0.3$ were lower than those at higher X_{R600a} , and these lower values resulted from high Ω_{tot} , as it is evident from the results in Fig. 5(a) for $T_{exp,in} = 190$ °C. This finding seems to show that the values of ζ and η_{II} are mainly affected by Ω_{tot} and Ψ_{loss} at the low and high

X_f , respectively.

A comparison between Figs. 5(b) and 4(b) shows that η_I , η_{II} , ζ , and Ω_{tot} were significantly related to condensation pressure and temperature glide because their profiles were similar to the trend of condensation pressure for R600a/R134a. Ω_{tot} was reduced by the condensation pressure associated with the mole fraction of the HCT fluid to cause an increase in ζ and η_{II} . Note that in comparison with the case of R600a/R1234yf, ζ , η_I , and η_{II} of R600a/R134a can be improved by temperature glide and $T_{exp,in}$. However, effects of $T_{exp,in}$ on η_I were slighter.

Figures 5(b), 5(c), and 5(d) reveal that the appearances of the first peak value of ζ , η_I , and η_{II} at $T_{exp,in} \leq 160^\circ\text{C}$ for X_{R600a} and $T_{exp,in} \leq 170^\circ\text{C}$ for X_{R245fa} were affected by the temperature glide when X_f was low. This was because Ω_{tot} was reduced to the lowest value when the temperature glide equaled the cooling source temperature increase. Meanwhile, at $T_{exp,in} \geq 170^\circ\text{C}$ for X_{R600a} and $T_{exp,in} \geq 180^\circ\text{C}$ for X_{R245fa} , two peak values of η_I , η_{II} , and ζ appeared at $X_f < 0.5$ and $X_f > 0.5$, respectively. Additionally, the trends of η_I and Ψ_{loss} are the same, that is, η_I and Ψ_{loss} reached their maximal values at $X_f = 1$, except when $T_{exp,in} \leq 160^\circ\text{C}$. This was because the condensation pressure and critical temperature of the mixtures reached the minimum and maximal values (referred to Figs. 3 and 4), respectively.

To further investigate the effects of the condensation pressure associated with the proportion of the HCT working fluid in the mixtures on total irreversibility, the irreversibilities of the main components of the TRC are shown in Fig. 6. For $T_g < \Delta T_{cs}$, the results show that Ω_{cond} and Ω_{pump} decreased obviously and slightly, respectively, with condensation pressure, which decreased with increasing X_f , as shown in Fig. 6(a). By contrast, Ω_{eva} and Ω_{exp} increased slightly with a decrease in condensation pressure. Meanwhile, Ψ_{loss} increased significantly with an increase in X_f owing to an apparent decrease in $\Delta \dot{E}_{hs}$. Moreover, Ω_{eva} and Ψ_{loss} were significantly affected by the critical temperature at the given expander inlet temperature. The maximal condensation temperature glide for R245fa/R1234yf was approximately 17°C , and as a result, the effects of condensation temperature glide occurred at $0.19/0.81$ ($X_{R245fa} < 0.5$) and $0.96/0.04$ ($X_{R245fa} > 0.5$) when the condensation temperature glide approached the increase in cooling source temperature. $\Delta \dot{E}_{hs}$, Ω_{exp} , Ω_{eva} , Ω_{cond} , and Ψ_{loss} were slightly and significantly affected by the condensation temperature glide, when $X_{R245fa} < 0.5$ and $X_{R245fa} > 0.5$ (Fig. 6(b)), respectively. In other words, the effects of temperature glide were evident when the mole fraction of the HCT fluid was high at $T_{exp,in}$ of 180°C and 190°C . This was because the lowest values of Ω_{cond} and Ψ_{loss} occurred at a high proportion of the HCT fluid and high $T_{exp,in}$ upon an effect of temperature glide.



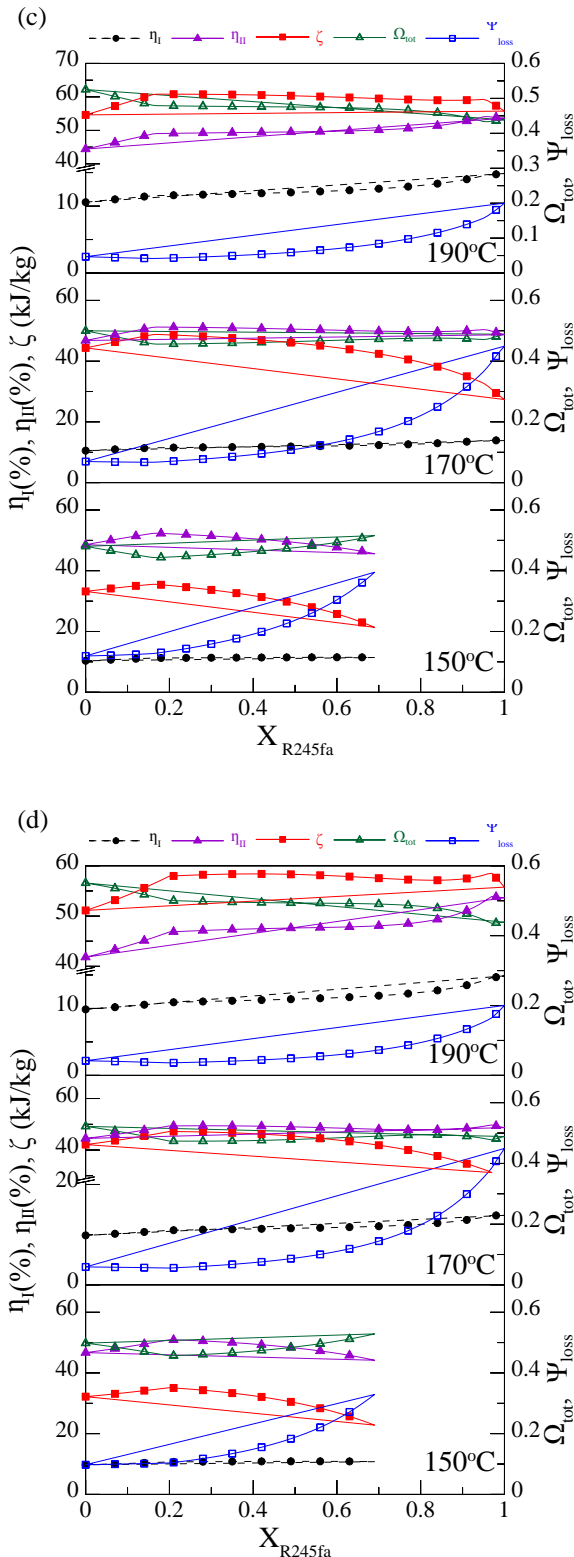


Fig. 5. Effects of inlet temperatures of the expander in the case of zeotropic mixture with $P_{exp,in} = 4.6$ MPa: (a) R600a/R1234yf, (b) R600a/R134a, (c) R245fa/R134a and (d) R245fa/R1234yf.

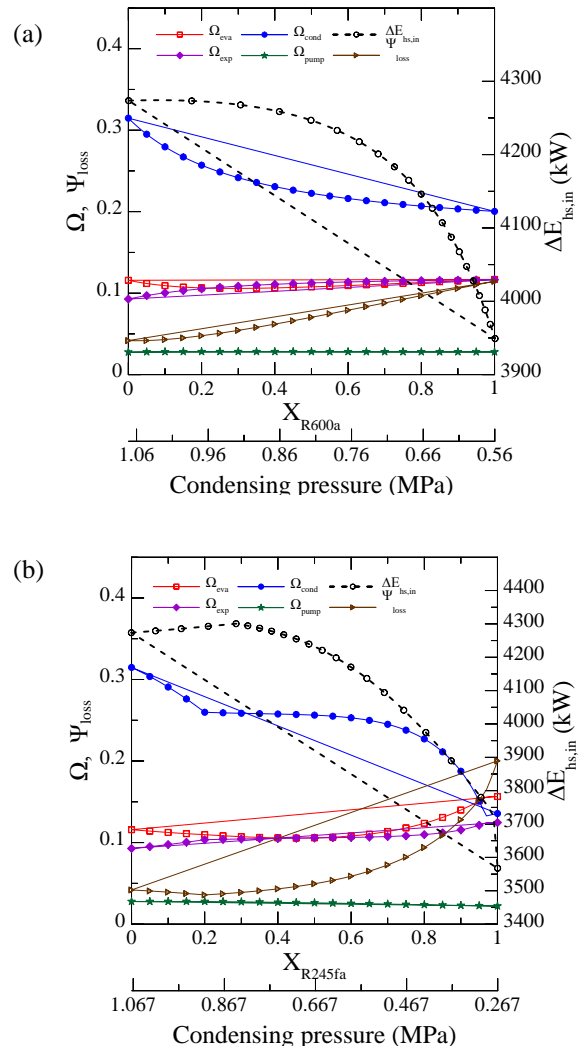


Fig. 6. Effects of condensing pressure on system performance, irreversibility, and exergy for (a) R600a/R1234yf and (b) R245fa/R1234yf at $T_{exp,in} = 190$ °C and $P_{exp,in} = 4.6$ MPa.

Influences of critical temperature and expander inlet temperature

To investigate the effects of the interaction between the expander inlet temperature and the critical temperature of the mixtures, the exergy loss and normalized irreversibilities of the components at various expander inlet temperatures are shown in Fig. 7. The results illustrate that the decreasing critical temperature and increasing expander inlet temperature were effective for reducing Ω_{eva} and Ψ_{loss} . At $\Delta T_{exp-crit} \geq 60$ °C, Ψ_{loss} approached a constant value lower than 0.05. This implies that the exergy from the heat source cannot attain its maximal value with a further decrease in the critical temperature and increase in the expander inlet temperature. Additionally, Ω_{eva} can attain its minimum value at $\Delta T_{exp-crit}$ ranging from 60 to 70 °C at the given $T_{exp,in}$. After Ω_{eva} reached its lowest value, it increased slightly with an increase in $\Delta T_{exp-crit}$. By contrast, the corresponding Ω_{cond} , which showed a trend opposite to those of Ω_{eva} and Ψ_{loss} , increased linearly

with $\Delta T_{\text{exp-crit}}$ at a given $T_{\text{exp,in}}$ owing to the higher condensation pressure of LCT fluids, as it is evident from the results in Fig. 7(d). Meanwhile, the crossover points of Ω_{eva} , Ω_{cond} , and Ψ_{loss} for the mixtures were in the $\Delta T_{\text{exp-crit}}$ range of 30 to 40 °C. After the crossover points, the slopes of Ω_{eva} and Ψ_{loss} decreased gradually.

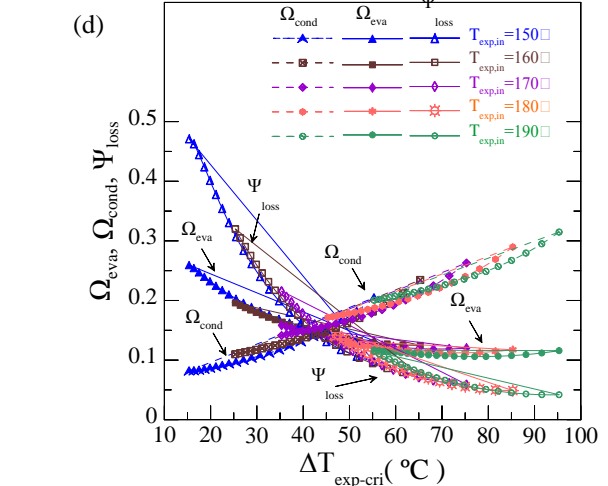
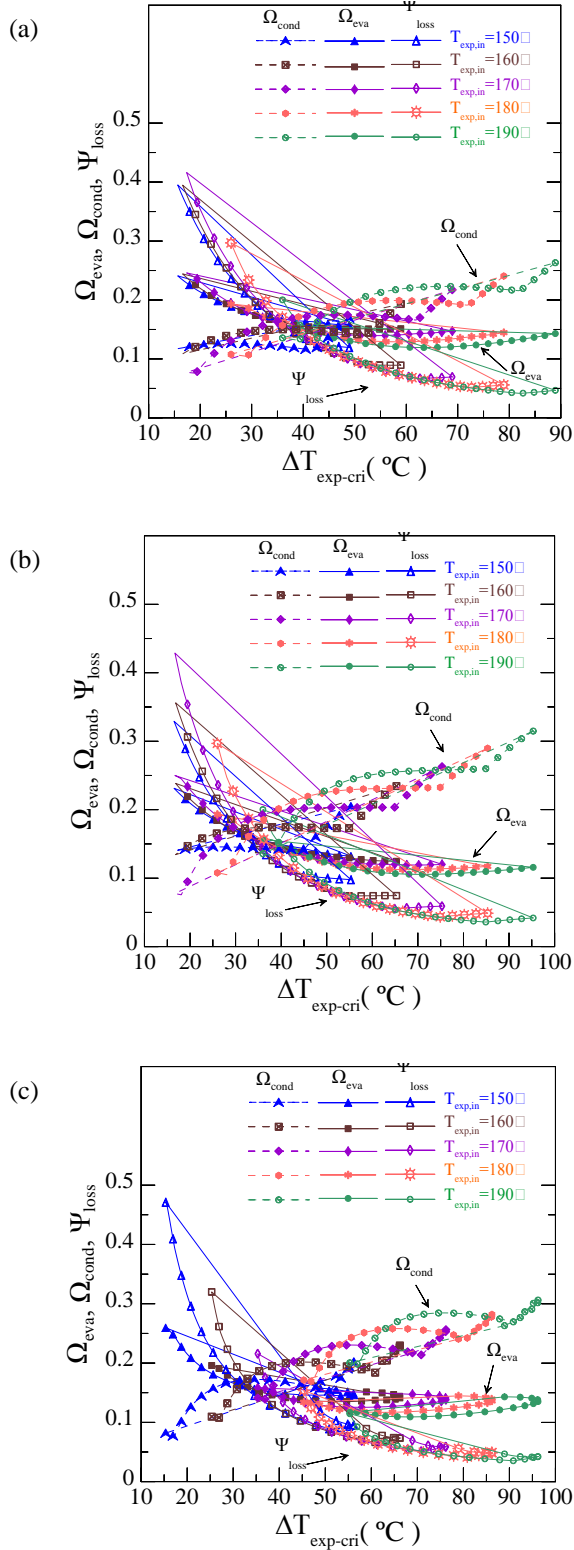


Fig. 7 Effects of $\Delta T_{\text{exp-crit}}$ at $P_{\text{exp,in}} = 4.6$ MPa for (a) R245fa/R134a, (b) R245fa/R1234yf, (c) R600a/R134a, and (d) R600a/R1234yf on the irreversibility and exergy loss.

Figure 8 shows how the η_I , η_{II} , and ζ of the system performance are associated with the mixtures influenced by $\Delta T_{\text{exp-crit}}$ at various inlet expander temperatures. The values of η_{II} were increased and decreased with inlet expander temperature as $\Delta T_{\text{exp-crit}}$ was lower and higher than 40 °C, respectively. Meanwhile, ζ was sharply and gradually increased with inlet expander temperature at $\Delta T_{\text{exp-crit}}$ lower and higher than 40 °C, respectively, except X_{R600a} . In other words, as $T_{\text{exp,in}} \leq 170$ °C and $T_{\text{exp,in}} \geq 180$ °C, the HCT fluid of the mixtures was selected as low and high proportion to obtain maximal values of ζ and η_{II} , respectively, upon the effects of temperature glide. A comparison of Figs. 7 and 8 shows that η_{II} for R245fa/R134a, R245fa/R1234yf, R600a/R134a and R600a/R1234yf were respectively reached their maximal values at 38.74, 38.07, 47.27 and 44.55 °C of $\Delta T_{\text{exp-crit}}$ as inlet expander temperatures of 190, 190, 180 and 170 °C, as listed in Table 4. Note that maximal η_{II} was occurred at high proportion of HCT fluids upon effect of condensation temperature glide when $\Delta T_{\text{exp-crit}}$ was approximately approached 40 °C. This can be considered as the universal condition for $\Delta T_{\text{exp-crit}}$ on the maximal η_{II} of the mixtures as $T_{\text{exp,in}} < 200$ °C. Additionally, η_I for X_{R600a} was decreased with an increase of the inlet expander temperature as $T_{\text{exp,in}} \geq 180$ °C. This was because Ω_{eva} increased with $\Delta T_{\text{exp-crit}}$, after Ω_{eva} reached the lowest value.

To explore the net-power-to-cost ratio of the mixtures for various $\Delta T_{\text{exp-crit}}$, the net output powers per unit UA (Λ) examined at various inlet expander temperatures are shown in Fig. 9. In all cases, Λ increased and decreased with the expander inlet temperature and $\Delta T_{\text{exp-crit}}$, respectively. Meanwhile, the maximum and minimum Λ of X_{R245fa} occurred at the HCT and LCT of the pure fluid for $T_{\text{exp,in}} \geq 180$ °C, respectively. The trends for Λ in the case of X_{600a} were similar to those in the case of X_{R245fa} . As clearly shown in Fig. 3(a), the lowest critical temperature of R600a/R134a is 93.68 °C

at the mole fraction of 0.18/0.82. Meanwhile, the minimum Λ occurs at the mole fraction R600a(0.19)/R134a(0.81). The critical temperature was observed to be related negatively to the output-power-to-cost ratio. The HCT fluid was useful for improving Λ at high expander inlet temperatures.

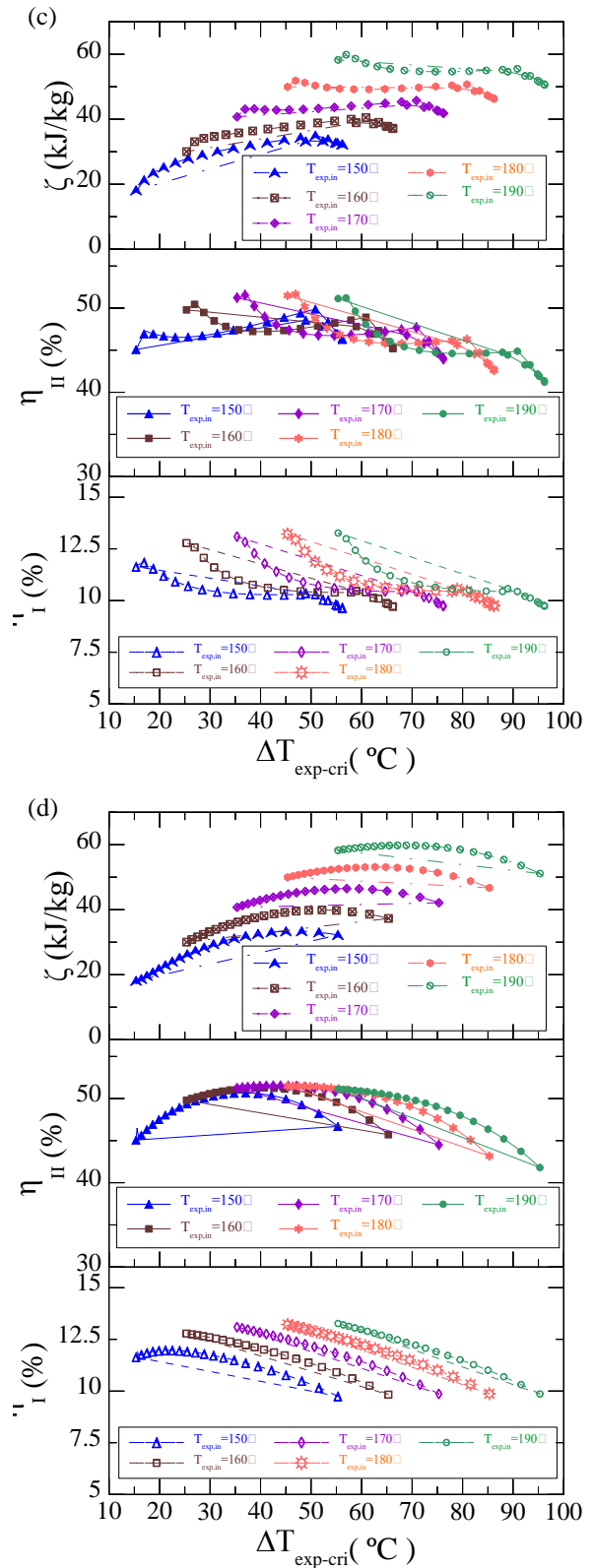
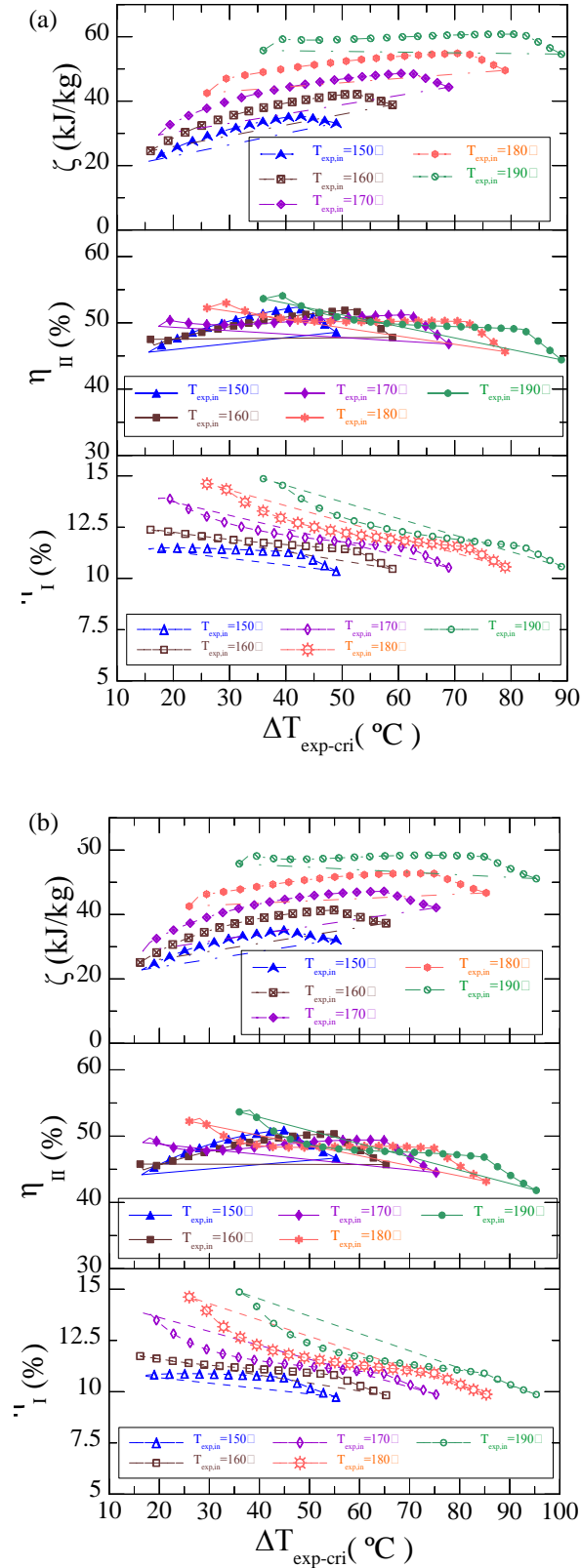


Fig. 8. Effects of $\Delta T_{exp-crit}$ at $P_{exp,in} = 4.6$ MPa for (a) R245fa/R134a, (b) R245fa/R1234yf, (c) R600a/R134a, and (d) R600a/R1234yf on the specific power, first and second law efficiencies.

Table 4 $\Delta T_{\text{exp-crit}}$ of mixtures on maximal value of η_{II} .

Mixtures	Mole fraction	$T_{\text{cri}} (\text{°C})$	$T_{\text{exp,in}} (\text{°C})$	$\Delta T_{\text{exp-crit}} (\text{°C})$	$\eta_{II} (\%)$
R245fa/R134a	0.96/0.04	151.26	190	38.74	54.60
R245fa/R1234yf	0.97/0.03	151.93	190	38.07	55.12
R600a/R134a	0.94/0.06	132.73	180	47.27	52.9
R600a/R1234yf	0.63/0.37	125.45	170	44.55	52.84

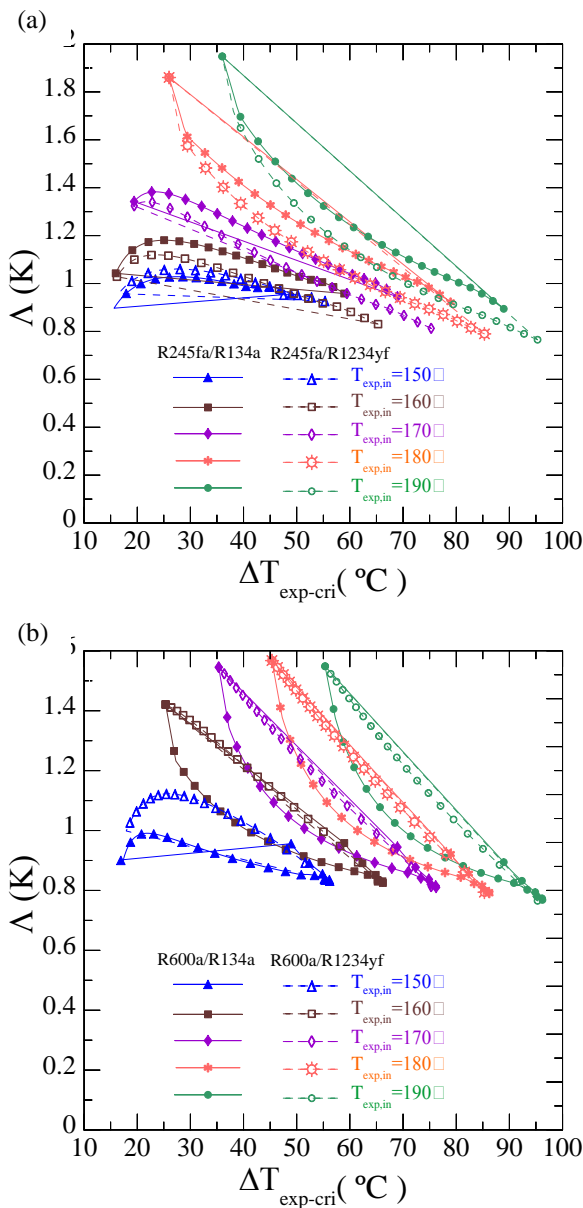


Fig. 9 Effects of $\Delta T_{\text{exp-crit}}$ on output power per unit UA at various expander inlet temperatures.

CONCLUSIONS

A thermodynamic analysis model of the TRC system associated with zeotropic mixtures was developed. R245fa/R134a, R245fa/R1234yf, R600a/R134a, and R600a/R1234yf were used as the mixture working fluids. The key results obtained herein can be summarized as follows:

1. The working fluids were mixed at the different critical temperatures of the pure refrigerants so that the critical temperatures of the mixtures could be adjusted in order to investigate exergy, irreversibility, and system performance at various expander inlet temperatures. In the present study, the TRC analysis model was validated against the results obtained in Le et al. (2014).
2. η_I and Ω_{cond} associated with the condensation pressure of the mixtures should be affected insignificantly by T_{cri} . Supposing that the proportion of the HCT fluid approaches 100%, then η_I and Ω_{cond} will achieve maximal and minimum values, respectively. Additionally, η_I was slightly affected by the expander inlet temperature.
3. After Ω_{eva} reached its lowest value, it increased slightly with an increase in $\Delta T_{\text{exp-crit}}$. By contrast, Ω_{cond} increased linearly with increasing $\Delta T_{\text{exp-crit}}$ at the given $T_{\text{exp,in}}$ owing to the effects of condensation pressure. At $\Delta T_{\text{exp-crit}} \geq 60$ $^{\circ}\text{C}$, Ψ_{loss} approached a constant value lower than 0.05.
4. The crossover points of Ω_{eva} , Ω_{cond} , and Ψ_{loss} were in the $\Delta T_{\text{exp-crit}}$ range of 30 to 40 $^{\circ}\text{C}$. Before crossover points, Ω_{eva} and Ψ_{loss} can be reduced effectively by decreasing T_{cri} of the mixtures and increasing $T_{\text{exp,in}}$. In the results, the values of ζ and η_{II} were significantly improved by Ψ_{loss} and Ω_{eva} , and by Ω_{cond} at $\Delta T_{\text{exp-crit}}$ higher and lower than 40 $^{\circ}\text{C}$ at the given inlet expander temperature, respectively. The high mole fraction HCT fluids of mixtures have the maximal η_{II} at crossover point associated with equilibrium of Ω_{eva} , Ω_{cond} , and Ψ_{loss} as $\Delta T_{\text{exp-crit}}$ approximately approached 40 $^{\circ}\text{C}$. A universal condition for $\Delta T_{\text{exp-crit}}$ was identified on the maximal η_{II} of the mixtures associated with high HCT

proportion as $T_{\text{exp,in}} < 200^\circ\text{C}$.

- For a low $T_{\text{exp,in}}$, η_{II} and ζ can achieve the peak values at the high proportion of the LCT fluid of the mixtures that resulted from a low Ω_{eva} and Ψ_{loss} upon an effect of temperature glide. By increasing the expander inlet temperature at a high proportion of the HCT fluid associated with low Ω_{cond} , Ω_{eva} and Ψ_{loss} can be significantly reduced to increase η_{II} and ζ to maximal values based on the effect of temperature glide. Meanwhile, the net-output power-to-cost ratio can be improved by increasing the proportion of the HCT fluid of the mixtures.

ACKNOWLEDGMENT

The authors gratefully acknowledge the financial support provided to this study by the Ministry of Science and Technology of the Republic of China under MOST106-2218-E-167-002-MY2, MOST108-2221-E-167-007-MY3 and MOST 110-2622-E-006-001-CC1, and the Higher Education SPROUT Project of the Ministry of Education of the Republic of China.

REFERENCES

- Wu, Y., Zhu, Y., and Yu, L., "Thermal and economic performance analysis of zeotropic mixtures for Organic Rankine Cycles," *Appl Therm Eng* Vol.96, pp.57-63(2016).
- Zhou, Y., Zhang, F., and Yu, L., "Performance analysis of the partial evaporating organic Rankine cycle (PEORC) using zeotropic mixtures," *Energy Convers Manag.*, Vol.129, pp.89-99(2016).
- Zhao, L. and Bao, J., "Thermodynamic analysis of organic Rankine cycle using zeotropic mixtures," *Appl Energy.*, Vol.130, pp.748-56(2014).
- Lecompte, S., Ameel, B., Ziviani, D., Broek, M. van den., and Paepe, MD., "Exergy analysis of zeotropic mixtures as working fluids in Organic Rankine Cycles," *Energy Convers Manag.*, Vol.85, pp.727-39(2014).
- Liu, Q., Duan, Y., and Yang, Z., "Effect of condensation temperature glide on the performance of organic Rankine cycles with zeotropic mixture working fluids," *Appl Energy.*, Vol.115, pp.394-404(2014).
- Zhou, Y., Zhang, F., and Yu, L., "The discussion of composition shift in organic Rankine cycle using zeotropic mixtures," *Energy Convers Manag.*, Vol.140, pp.324-33(2017).
- Aghahosseini, S. and Dincer, I., "Comparative performance analysis of low-temperature Organic Rankine Cycle (ORC) using pure and zeotropic working fluids," *Appl Therm Eng.*, Vol.54, pp.35-42(2013).
- Zhai, H., An, Q., and Shi, L., "Analysis of the quantitative correlation between the heat source temperature and the critical temperature of the optimal pure working fluid for subcritical organic Rankine cycles," *Appl Therm Eng.*, Vol.99, pp.383-91(2016).
- Heberle, F., Preißinger, M., Brüggemann, D., "Zeotropic mixtures as working fluids in Organic Rankine Cycles for low-enthalpy geothermal resources." *Renew Energy.*, Vol.37, pp.364-70(2012).
- Wang, XD. and Zhao, L., "Analysis of zeotropic mixtures used in low-temperature solar Rankine cycles for power generation." *Solar Energy.*, Vol.83, pp.605-13(2009).
- Satanphol, K., Pridasawas, W., and Suphanit, B., "A study on optimal composition of zeotropic working fluid in an Organic Rankine Cycle (ORC) for low grade heat recovery." *Energy.*, Vol.123, pp.326-39(2017).
- Hsieh, J.C. and Cheng, CH., "Effects of evaporation parameters on recuperative transcritical organic Rankine cycle using binary mixture fluids," *International Journal of Low-Carbon Technologies.*, Vol.16, pp.275-286(2021).
- Schuster, A., Karellas, S., and Aumann, R., "Efficiency optimization potential in supercritical Organic Rankine Cycles." *Energy.*, Vol.35, pp.1033-39(2010).
- Chen, H., Goswami, DY., Rahman, MM., Stefanakos, EK. "Energetic and exergetic analysis of CO₂- and R32-based transcritical Rankine cycles for low-grade heat conversion." *Appl Energy.*, Vol.88, pp.2802-08(2011).
- Algieri, A. and Morrone, P., "Comparative energetic analysis of high-temperature subcritical and transcritical Organic Rankine Cycle (ORC): A biomass application in the Sibari district." *Appl therm Eng.*, Vol.36, pp.236-24(2012).
- Le, VL., Feidt, M., Kheiri, A., "Pelloux-Prayer S. Performance optimization of low-temperature power generation by supercritical ORCs (organic Rankine cycles) using low GWP (global warming potential) working fluids." *Energy.*, Vol.67, pp.513-26(2014).
- Mehrpooya, M., Bahramian, P., Pourfayaz, F., Rosen, MA., "Introducing and analysis of a hybrid molten carbonate fuel cell-supercritical carbon dioxide Brayton cycle system." *Sustain Energy Techn.*, Vol.18, pp.100-06(2016).
- Wu, C., Wang, SS., Jiang, X., and Li, J., "Thermodynamic analysis and performance optimization of transcritical power cycles using CO₂-based binary zeotropic mixtures as working fluids for geothermal power plants." *Appl Therm Eng.*, Vol.115, pp.292-304(2017).
- Wang, X. and Dai, Y., "Exergoeconomic analysis of utilizing the transcritical CO₂ cycle and the ORC

- for a recompression supercritical CO₂ cycle waste heat recovery: A comparative study.” *Appl Energy*, Vol.170, pp.193-207(2016).
- Liu, P., Shua, G., Tian, H., Feng, W., Shi, L., and Wang, X., “Experimental study on transcritical Rankine cycle (TRC) using CO₂/R134a mixtures with various composition ratios for waste heat recovery from diesel engines.” *Energy Convers Manage.*, Vol. 208(2020).
- Song, J., Li, X., Ren, X., Tian, H., Shu, G., Gu, C., and Markides, CN., “Thermodynamic and economic investigations of transcritical CO₂-cycle systems with integrated radial-inflow turbine performance predictions.” *Appl Energy*, Vol.165, pp.11464(2020).
- Hsieh, JC. “Effect of heat extraction optimization with supercritical carbon dioxide on transcritical power cycle,” *Int J Energy Res.*, Vol.44, pp.5806-5818(2020).
- Zhi, LH., Hu, P., Chen, LX., and Zhao, G., “Multiple parametric analysis, optimization and efficiency prediction of transcritical organic Rankine cycle using trans-1,3,3,3-tetrafluoropropene (R1234ze(E)) for low grade waste heat recovery.” *Energy Convers Manage.*, Vol.180, pp.44-59(2019).
- Dai, B., Li, M., and Ma, Y., “Thermodynamic analysis of carbon dioxide blends with low GWP (global warming potential) working fluids-based transcritical Rankine cycles for low-grade heat energy recovery.” *Energy*, Vol.64, pp.942-52(2014).
- Braimakis, K., Preißinger, M., Brüggemann, D., Karellas, S., and Panopoulos, K., “Low grade waste heat recovery with subcritical and supercritical Organic Rankine Cycle based on natural refrigerants and their binary mixtures.” *Energy*, Vol.88, pp.80-92(2015).
- Chen, H., Goswami, DY., Rahman, MR., and Stefanakos, EK., “Energetic and exergetic analysis of CO₂- and R32-based transcritical Rankine cycles for low-grade heat conversion.” *Appl Therm Eng.*, Vol.88, pp.2802-08(2011).
- Wu, Y., Zhu, Y., and Yu, L., “Thermal and economic performance analysis of zeotropic mixtures for Organic Rankine Cycles.” *Appl Therm Eng.*, Vol.96, pp.57–63(2016).
- Le, VL., Kheiri, A., Feidt, M., and Pelloux-Prayer, S., “Thermodynamic and economic optimizations of a waste heat to power plant driven by a subcritical ORC (Organic Rankine Cycle) using pure or zeotropic working fluid.” *Energy*, Vol.78, pp.622-38(2014).
- Maraver, D., Royo, J., Lemort, V., and Quoilin, S., “Systematic optimization of subcritical and transcritical organic Rankine cycles (ORCs) constrained by technical parameters in multiple applications.” *Appl Energy*, Vol.117, pp.11-29(2014).
- Hsieh, JC., Fu, BR., Wang, TW., Cheng, Y., Lee, YR., and Chang, JC., “Design and preliminary results of a 20-kW transcritical organic Rankine cycle with a screw expander for low-grade waste heat recovery.” *Appl Therm Eng.*, Vol.110, pp.1120–27(2017).
- Lemmon, EW., Huber, ML., McLinden, MO., NIST Standard Reference Database 23: Reference Fluid Thermodynamic and Transport Properties REFPROP, Version 9.1, National Institute of Standards and Technology, Standard Reference Data Program, Gaithersburg, USA, 2013.

NOMENCLATURE

- \dot{m} : mass flow rate (kg/s)
- \dot{E} : exergy (W)
- e : specific exergy (kJ/kg)
- f : front
- g : glide
- h : specific enthalpy (kJ/kg)
- \dot{I} : irreversibility (W)
- HCT : high critical temperature (°C)
- LCT : low critical temperature (°C)
- $LMTD$: log mean temperature difference (°C)
- P : pressure (Pa)
- \dot{P} : electric power (W)
- Q : power (W)
- s : specific entropy (kJ/kg · K)
- T : temperature (°C)
- UA : overall heat transfer coefficient
- \dot{W} : mechanical power (W)
- X : mole fraction
- Greek symbols**
- Δ : difference
- ε : efficiency (%)
- ζ : specific power (kJ/kg)
- η : thermal efficiency (%)
- Λ : net output powers per unit UA (K)
- Ψ : normalized exergy
- Ω : normalized irreversibility

Subscript

cond: condenser
cri: critical point
cs: cooling source
eva: evaporator
exp: expander
f: working fluid
g: generator
hs: heating source
I: first
II: second
in: inlet
input: input
is: isentropic
loss: loss
m: mechanical
net: net
out: outlet
pp: pinch point
sys: system
th: thermal
tot: total

Abbreviation

ANN: artificial neural network
GWP: global warming potential
HC: hydrocarbon
HCT: high critical temperature
HFO: hydrofluoroolefin
LCT: low critical temperature
NIST: National Institute of Standards and Technology
ORC: organic Rankine cycle
PEORC: partial evaporating organic Rankine cycle
TRC: transcritical organic Rankine cycle

在低階熱源下非共沸混合流體之臨界溫度對穿臨界有機朗肯循環之能量與可用能影響

謝瑞青 黃定璿

國立勤益科技大學機械工程系

摘要

本研究開發非共沸混合物相關的跨臨界有機朗肯循環的熱力學分析模型。該模型用於研究在膨脹機入口溫度 150–190 °C，臨界混合物溫度對熱力學第一和第二定律效率、比功、淨功率成本比、元件的不可逆性以及熱源的可用能損失之影響。結果表明，隨著膨脹機入口溫度的升高和混合物臨界溫度的降低，蒸發器的不可逆性和熱源的火用損失顯著降低，從而提高了比功和第二定律效率。然而，由於低臨界溫度流體的冷凝壓力的影響，冷凝器不可逆性隨著混合物臨界溫度的降低而增加。在分析的基礎上，提出了臨界溫度與膨脹機入口溫度之間的溫差對最大第二定律效率的通用準則。最後，混合流體的高臨界溫度伴隨著低冷凝壓力，導致高第一定律效率、低冷凝器不可逆性和優異的淨功率成本比。